THERMAL MODELING AND EXPERIMENTAL TECHNIQUES FOR MICROWAVE BIPOLAR DEVICES

K.J. Negus and R.W. Franklin
Advanced Bipolar Products
Avantek, Inc.
39201 Cherry St.
Newark, CA, 94560

and

M.M. Yovanovich
Microelectronics Heat Transfer Laboratory
University of Waterloo
Waterloo, Ontario
CANADA, N2L 3G1

Abstract - Many thermal issues facing the microwave bipolar industry are discussed in this paper and the application of experimental and modeling techniques is demonstrated for real microwave devices. The liquid crystal transition method of thermal measurement is shown to be useful for modern bipolar devices because the method can resolve temperatures with excellent spatial resolution. Infra-red detection, however, generally does not have the necessary resolution for modern small geometry devices. An experimental technique for determining thermal resistance from device terminal characteristics is also shown to be adequate for some applications and packages. Thermal analysis through the use of an exact solution to a three-dimensional model of the semiconductor die is also presented in this paper. The modeling technique compares extremely well with detailed measurements by liquid crystal transition on microwave bipolar devices. The application of experimental and analytical thermal characterization is discussed and shown to be important for problems such as device optimization and reliability predictions.

Introduction

Accurate thermal characterization of semiconductor devices both in die form and in packages is important to the microwave industry for several reasons. First, the thermal resistance from junction to ambient is required to predict the correct device temperature and subsequently the device electrical performance in different environments. And second, the thermal resistance must be known to accurately extrapolate product lifetime predictions from high temperature accelerated failure tests with normal electrical bias conditions. Furthermore, with bipolar transistors a destructive mechanism known as thermal runaway or second breakdown can occur under some bias conditions even when the junction temperature is only 20 $^{\circ}C$ above ambient [1]. Finally accurate thermal characterization can aid in device layout and packaging for optimum power dissipation capability.

The microwave industry has for many years used a variety of experimental methods such as infra-red detection [13], liquid-crystal transition [14] and ideal junction law assumptions to measure thermal resistance [15]. These methods each have their own advantages and disadvantages but all three can be useful for characterizing bipolar devices. Numerical thermal analysis techniques have been available recently but are still limited by the complexity of the heat conduction within the die and the conduction, convection and/or radiation mechanisms within the package and external system.

The microwave devices of interest in this work can be considered thermally different from most commercial integrated circuit (IC) products because a significant or dominant fraction of their overall thermal resistance is due to heat conduction within the die. With microwave bipolar devices the semiconductor die is quite small relative to its package which is often made of a high conductivity material such as beryllia (BeO). Furthermore, the heat generation within the die is usually concentrated in one or several small regions of high local power dissipation and thus significant temperature variations can occur over large power devices or between different devices in Monolithic Microwave Integrated Circuits (MMIC's). The thermal resistance within the die is also strongly affected by the extreme negative temperature dependence of thermal conductivity for most semiconductors including silicon and gallium arsenide. Microwave devices are also thermally different from many large power switching transistors because the local power dissipation densities are higher and concentrated in smaller active regions.

Thermal analysis software can aid greatly both to characterize these die temperature variations and to optimize new device structures. For a microwave semiconductor device manufacturer, thermal analysis of the die can thus lead to product improvements due to die thickness or device layout changes. In this paper the theory, usage and experimental validation is described for the thermal analysis program THEATRIC (THErmal Analysis of TRansistors and Integrated Circuits) [2,3]. A variety of commercially-available finite element or finite volume codes could also be used for this purpose but they require considerable computing resources and engineering effort. THEATRIC is an IBM PC-based software program which utilizes the Surface Element Method and the Method of Infinite Images to analytically solve the non-linear three-dimensional problem of heat flow within a semiconductor die. The program has a menu-driven graphical interface and rapid typical execution times on a microcomputer.

Obviously, validation of modeling software through experiments is desirable to develop faith in the information gained from computer analysis. Additionally though, the combination of modeling and experiment can help in characterizing products where direct thermal measurement is difficult, in studying the impact of process and assembly variations and in extrapolating low temperature thermal resistance measurements correctly for high temperature reliability studies.

CH2688-0/89/0000-0063 $1.00 © 1989 IEEE

Thermal Issues with Typical Microwave Devices

In this work thermal modeling and experimental techniques are discussed with particular emphasis on microwave silicon bipolar transistors and small-scale silicon bipolar MMIC's. Although most of this material should apply equally well for discrete gallium arsenide MESFET's and gallium arsenide MMIC's, it is important to distinguish the devices of interest in this work from the majority of commercial IC's such as memory chips or gate arrays.

An example of a small-scale silicon bipolar MMIC is the A08 MODAMP^{tm} from Avantek shown in a the cavity of a 100 mil stripline package in Figure 1. Note that this die is only 394 $\times$ 305 $\times$ 114 μm in size. Furthermore the majority of the power dissipation (typically about 300 mW) is realized in two small rectangular regions located in the lower left corner of the die as orientated in Figure 1. Not only is this die small relative to its package, but also the 100 mil stripline package itself is quite small as shown in Figure 2 by the comparison of typical microwave packages versus a pin grid array package and a ceramic dual-inline package. In Figure 2 the 100 mil stripline package is the smaller four-leaded package located next to the pin grid array package. A typical value of thermal resistance from junction to case (θ_{jc}) for the product shown in Figure 1 is 200 $°C/W$ of which about 100 $°C/W$ is due to conduction within the die and 100 $°C/W$ due to the package. Other packages used for such products have considerably lower thermal resistance. For example, a 230 mil BeO flange package contributes about 5 $°C/W$ to θ_{jc} (this package is the largest microwave package shown in Figure 2). In contrast, an ECL logic chip measuring 3 mm on a side and located in a 28 pin ceramic quad with forced-air cooling might have a θ_{jc} of about 20 $°C/W$ of which only 2–3 $°C/W$ is usually due to heat conduction within the die.

For a microwave semiconductor manufacturer, therefore, the analysis and measurement of the temperature distribution on the actual die is important. This is especially true for MMIC's where several active power dissipation regions can thermally interact with each other and have device temperature differences on die which cause degradation of electrical circuit performance. Most bipolar devices are also ultimately limited for long-term reliability by metal electromigration failures which occur at points of high temperature, high temperature gradient and high current density. These points are not always at the maximum die temperature nor are they always related to the best "equivalent" temperature used to predict terminal characteristics from standard electrical device models. Thus for many microwave bipolar devices the actual definition of thermal resistance θ_{jc} can be somewhat ambiguous depending on the end usage of the number and the measurement technique used to obtain it.

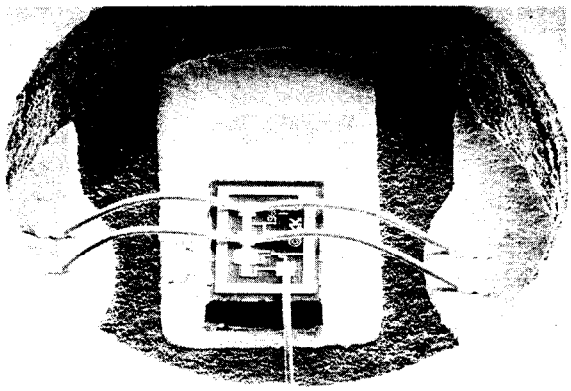

Figure 1: Avantek MODAMP^{tm} in 100 mil Stripline Package

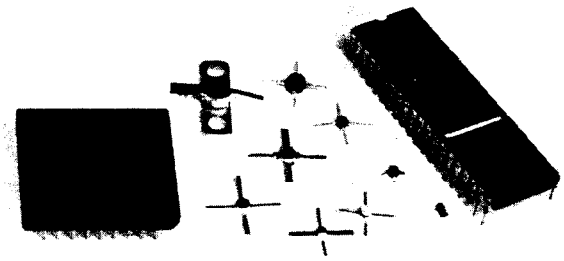

Figure 2: Comparison of Avantek Microwave Packages with a Pin Grid Array Package (far left) and a Ceramic Dual-Inline Package (far right)

Experimental Techniques

Infra-Red Detection

The microelectronics industry has often found infra-red (IR) detection to be a valuable tool for thermal characterization of surfaces at the die, package and cooling system levels. In fact, manufacturers of large power bipolar transistors often find IR detection useful to identify hot spots due to poor die attach and/or non-uniform current distribution.

IR detection has several major advantages over other thermal measurement techniques. First, the method is basically non-intrusive which is critical for small systems. And second, IR detection provides a "complete" picture or map of the surface temperature over its field of view just as a thermal analysis program would provide. Thus localized hot spots and high temperature gradients are easily identified. IR detection can also be calibrated to work over a variety of temperature ranges and is easily automated with a computer for data reduction.

Unfortunately though, one major disadvantage restricts the utility of IR detection for thermal characterization of typical microwave bipolar devices. The limitation is its inablility to resolve thermal gradients across the very small distances (less than 5 μm) needed to thermally characterize high performance bipolar devices. For example at Avantek, IR detection is commonly used to measure large power devices and hybrid circuits. When applied, however, to small geometry bipolar devices where the active emitter fingers are on 4 μm centers and are 25 μm or less in length, the present IR resolution limit of around 15 μm leads to gross, non-repeatable underpredictions of θ_{jc}.

Other disadvantages of IR detection include its relatively high cost and its inability to characterize plastic packages where the die surface cannot be optically isolated under bias.

Liquid Crystal Transition

The thermal measurement technique of liquid crystal transition (LCT) shares some features in common with IR detection in that it is applied to the measurement of surface temperatures on surfaces which can be optically isolated. Unlike IR detection, LCT has the significant restriction that only a single temperature transition on the surface can be detected for a given liquid crystal coating. However, LCT has much greater resolution for small active devices (essentially optical resolution – easily able to detect temperature changes over distances of 2–4 μm) and is thus preferable for small geometry microwave bipolar devices and silicon MMIC's. In many cases the inability of LCT to show a

complete map of surface temperatures can be overcome through accurate correlation to a modeling program such as THEATRIC (this is illustrated later in this work).

The increased resolution of LCT measurement allows the problem of θ_{jc} definition to be addressed for different applications such as electromigration-induced reliabilty studies, overall average device temperatures, and maximum die surface temperature (limiting factor for plastic packages). In addition the excellent resolution identifies problems such as "current hogging" (which can lead to thermal runaway) and "dead emitters" (due to poor electrical contacts).

The liquid crystal method of measuring the surface temperature of the die makes use of the temperature sensitivity of birefringent nematic liquid crystals [16]. On melting, liquid crystals do not form isotropic liquids directly, but pass through one or more intermediate states of order, as the order is lost in a reversible, stepwise manner over a range of temperature. This intermediate, or mesomorphic, state, may include up to three phases, depending on temperature: cholesteric (most ordered), smectic and nematic (least ordered). These mesomorphic phases, which appear as turbid, birefringent fluids, are ordered on a molecular level to varying degrees with the associated viscosities ranging from that of a paste to that of a freely flowing liquid.

This paper considers only the transition temperature at which a liquid crystal with a nematic mesophase changes to the isotropic liquid phase (the NI transition). The birefringence of the nematic mesophase can alter the polarization of an incident light beam whereas the the randomness of the isotropic liquid phase will not. Therefore a microscope system with crossed linear polarizers in the incident beam and ocular system will produce isotropic regions to appear darker than nematic regions. The boundary between the two regions will be at the NI transition temperature which can be calibrated separately.

A photograph of an example experimental set-up for LCT is shown in Figure 3. The liquid crystals, which are solid at room temperature, are first dissolved in an organic solvent such as acetone or Freon and then applied with a dropper. After the solvent evaporates, a layer of the liquid crystal is left coating the die surface. The coating is allowed to dry since the presence of solvent or water in the liquid crystal layer can alter the N-I transistion temperature. Ideally a calibration test of the mixture transistion temperature should be made. The region(s) of interest on the semiconductor die surface are then examined under a microscope while the bias to the active devices and the case temperature are varied. With suitable measurements of the total current and voltage supplied to the die (and hence power dissipation) and the case temperature (with a small thermocouple) the "growth" of the LCT region can be monitored as a function of power dissipation.

An example LCT measurement for a silicon MMIC, the Avantek INA-01, is shown in Figure 4. For this die four transistors are shown but the majority of power dissipation occurs on the output transistor located on the far right in Figure 4. At this particular bias and case temperature the LCT contour is seen to extend across most of the active area of the output transistor. Note that LCT contours are also completely covering the resistors immediately to the right of the output device. In fact the contour on the resistors appeared initially at lower power dissipation than that required to start the contour on the active device. For MMIC's in hermetic ceramic packages, the presence of hotter resistors than transistors may be of little concern if current densities remain acceptable in the resistors. However, the excessive heating of resistors could limit the safe operating temperature range for these products in plastic packages. Based

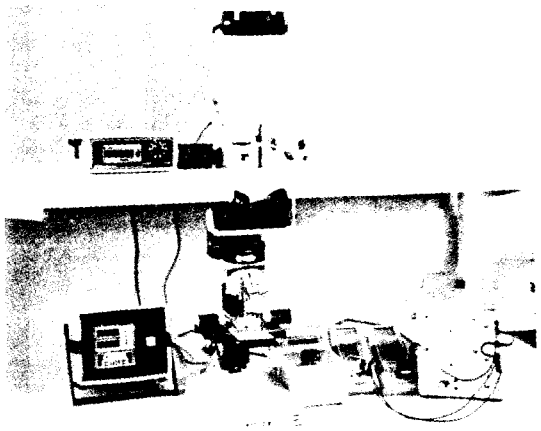

Figure 3: Liquid Crystal Set-up used at Avantek

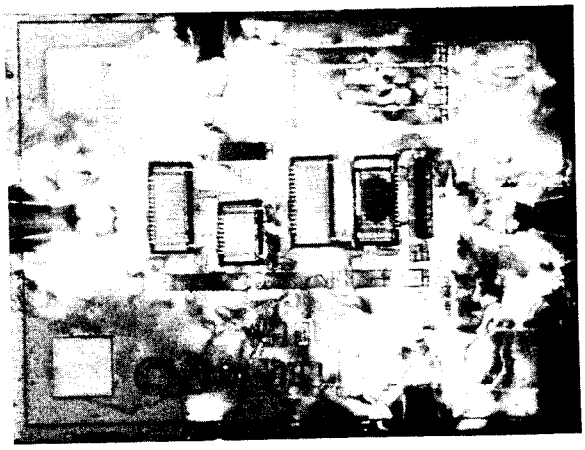

Figure 4: LCT Results for Avantek INA-01 MMIC at 100 $°C$

on the LCT results for this INA-01 at a transistion temperature of 100 $°C$, the thermal resistance θ_{jc} is approximately 80 $°C/W$ in the 230 mil BeO flange package.

Ideal Junction Law

A third technique used to thermally characterize microwave bipolar devices utilizes well-understood electrical device models of bipolar transistor terminal characteristics to infer a thermal resistance θ_{jc}. This method has some excellent advantages in that the θ_{jc} predicted is ideal for electrical device modeling purposes, the method does not need to destroy the die or package (ie. could be used for high reliability screening), the method does not require expensive θ_{jc}-specific equipment, and the method can be used on plastic packages. However, this technique also requires accurate knowledge of the electical operating characteristics of the individual device under test and provides no information whatsoever on the temperature distribution over the active device region(s). Furthermore, it is applicable mainly for discrete bipolar devices only and is difficult to extend to MMIC's. Note that this method is considerably different than using diode-based thermal test dice where the temperature-sensitive device and the power dissipation regions are biased separately.

The theoretical basis for the technique applied to a bipolar transistor biased as shown in Figure 5 starts by assuming that the device is operated in the forward active region where the collector current is well-approximated by the expression [4]

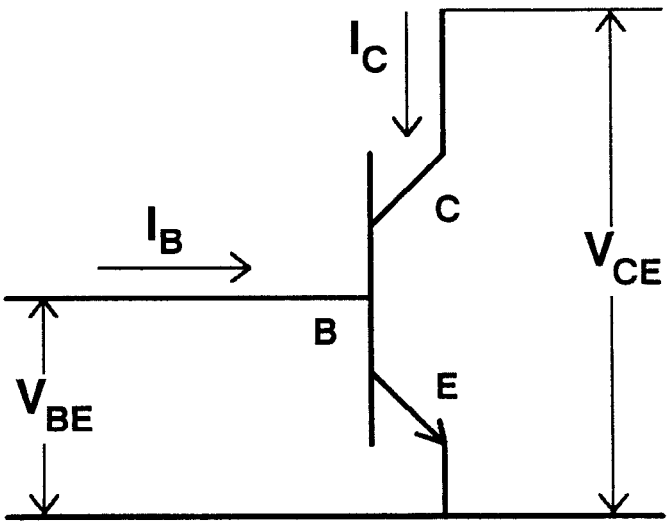

Figure 5: Bias Conditions for Ideal Junction Law Method

$$I_C = KT_j^n \exp\left[\frac{\lambda\,(V_{BE} - V_G)}{mT_j}\right] \tag{1}$$

where K is a constant which is a weak function of V_{CE}, T_j is the "equivalent" emitter-base junction temperature, V_G is the bandgap voltage which is a very weak function of T_j but independent of bias, n and m are modeling parameters, and λ is a physical constant ($\lambda = 1.16 \times 10^4\ °C/V$). Under the usual condition of $I_C \gg I_B$ then the total power dissipation is

$$Q = I_C V_{CE} \tag{2}$$

One might consider testing a given type of device with LCT to calibrate the modeling parameters K, n and m of eqn. (1) for values of T_j. However, for production microwave bipolar devices these parameters vary far too significantly from device to device, wafer to wafer and lot to lot to ever infer T_j accurately from measured terminal characteristics. Nonetheless, eqn. (1) can be utilized for measuring θ_{jc} very simply by making two measurements.

First, the device is biased at some V_{CE1}, I_{C1} and V_{BE1} using a transistor bias source and the case temperature T_{C1} is recorded. The transistor bias source then applies a second bias of V_{CE2} (still within the forward active region) and I_{C2} where $I_{C2} = I_{C1}$. The case temperature T_{C2} is then adjusted externally by varying the ambient temperature in a test chamber until $V_{BE2} = V_{BE1}$. It then follows logically from eqn. (1) that if K, n, m and V_G are not functions of V_{CE} (the only bias that changed), the junction temperatures T_{j1} and T_{j2} must be identical. If the thermal resistance from junction to case is defined as

$$\theta_{jc} = \frac{T_j - T_{C1}}{I_C V_{CE1}} = \frac{T_j - T_{C2}}{I_C V_{CE2}} \tag{3}$$

where $T_j = T_{j1} = T_{j2}$ and $I_C = I_{C1} = I_{C2}$, then the "equivalent" junction temperature is

$$T_j = \frac{V_{CE1}T_{C2} - V_{CE2}T_{C1}}{V_{CE1} - V_{CE2}} \tag{4}$$

and the junction to case thermal resistance is

$$\theta_{jc} = \frac{T_{C2} - T_{C1}}{I_C(V_{CE1} - V_{CE2})} \tag{5}$$

The are several major criticisms made against this method in addition to its obvious disadvantages of no temperature distribution and restriction to single bipolar transistors. First, the power dissipation varies from the first measurement to the second which can lead to inaccuracies due to the non-linearity of heat conduction in silicon (discussed in greater detail later in this paper). Second, the method requires blind faith that eqn. (1) is applicable in a given situation for those with little or no background in bipolar device physics. And finally, even when eqn. (1) is applicable, it is well known that the parameter K has a weak but non-negligible dependence on V_{CE} especially for modern high frequency transistors which have low Early voltages.

Despite these limitations though, the simplicity of the technique and its ability to measure θ_{jc} for real microwave devices in plastic packages makes it still attractive. Note additionally that eqn. (5) for computing θ_{jc} is given in terms of temperature and voltage *differences* at a fixed current. These quantities can all be measured very accurately even for small changes (ie. even if the thermocouple does not read absolute temperature with great accuracy it should still measure the temperature difference from one case to a second quite accurately). Furthermore, the dependence of the modeling parameter K on V_{CE} can be easily included in the experiment by recognizing that in the forward active range

$$K = K_0\left(1 + \frac{V_{CE}}{V_A}\right) \tag{6}$$

where K_0 is extremely insensitive to V_{CE} for a given I_C and V_A is the Early Voltage of the device which can be extracted easily with a curve tracer [5]. Thus when the second measurement in the experiment is taken, for $T_j = T_{j1} = T_{j2}$ and $I_C = I_{C1} = I_{C2}$, eqn. (1) requires

$$\left(1 + \frac{V_{CE1}}{V_A}\right)\exp\left[\frac{\lambda V_{BE1}}{mT_j}\right] = \left(1 + \frac{V_{CE2}}{V_A}\right)\exp\left[\frac{\lambda V_{BE2}}{mT_j}\right] \tag{7}$$

Rearranging this expression after substituting eqn. (4) for T_j then leads to the requirement that instead of $V_{BE2} = V_{BE1}$, the second measurement should be performed when T_{C2} is adjusted by the ambient conditions so that

$$V_{BE2} = V_{BE1} - \frac{m}{\lambda}\left[\frac{V_{CE1}T_{C2} - V_{CE2}T_{C1}}{V_{CE1} - V_{CE2}}\right]\ln\left(\frac{V_A + V_{CE2}}{V_A + V_{CE1}}\right) \tag{8}$$

In this case the experiment must now be performed in a bias range where m has a known value (usually where m is close to unity) from a Gummel plot [5]. Once eqn. (8) is satisfied then θ_{jc} is given as before by eqn. (5).

Table 1 summarizes some example results obtained using the ideal junction law technique for the Avantek 414 discrete microwave bipolar transistor in three different packages. For comparison purposes the estimated thermal resistances based on "average" device temperature obtained by LCT are also given for the two ceramic packages. The agreement between the ideal junction technique with the simple Early effect correction of eqn. (8) and the LCT method is excellent. The 230 mil BeO package is far superior thermally because it has a beryllia base and copper leads as opposed to the alumina base and kovar leads of the 100 mil Stripline package. For the plastic packages which represent the dominant portion of commercial sales, the corrected ideal junction technique may be the best method currently available and an example result for the 85 mil diameter Plastic package is given in Table 1. Note that although the plastic package has lower θ_{jc} due to its copper leads, the alumina stripline packages may still permit a higher ambient temperature because they are not limited to 150 $°C$ maximum die temperature.

Table 1: θ_{jc} Measurements of Avantek 414 Discrete Transistor

Package	θ_{jc} (°C/W)		
	Liquid Crystal	$V_{BE2} = V_{BE1}$	V_{BE2} from eqn. (8)
230 mil BeO Flange	95	140	105
100 mil Stripline	200	230	190
85 mil Plastic	-	185	145

Analytical Modeling – THEATRIC

As mentioned previously, the thermal modeling technique advocated in this work is based on an exact analytical solution to a non-linear three-dimensional model for heat conduction in a semiconductor die. The associated computer program is called THEATRIC based on THErmal Analysis of TRansistors and Integrated Circuits. Only a brief summary of THEATRIC's theoretical basis is given here since substantial explanations and derivations have been given elsewhere [2,3,6,7].

For most microwave bipolar applications, heat transfer from the semiconductor die is dominated by conduction through the die and into a high conductivity base (and then into some external cooling system). Heat flow from the top surface of the die by modes such as cavity conduction/radiation and bond wire conduction has been shown to be negligible for the devices of interest [3] and thus the top surface and sides of the die are modeled as adiabatic. The base of the die is modeled as an isotherm, $T = T_b$, as shown in Figure 6 where T_b is related to the total heat dissipation and external thermal resistance. The governing differential equation and boundary conditions with reference to Figure 6 are thus

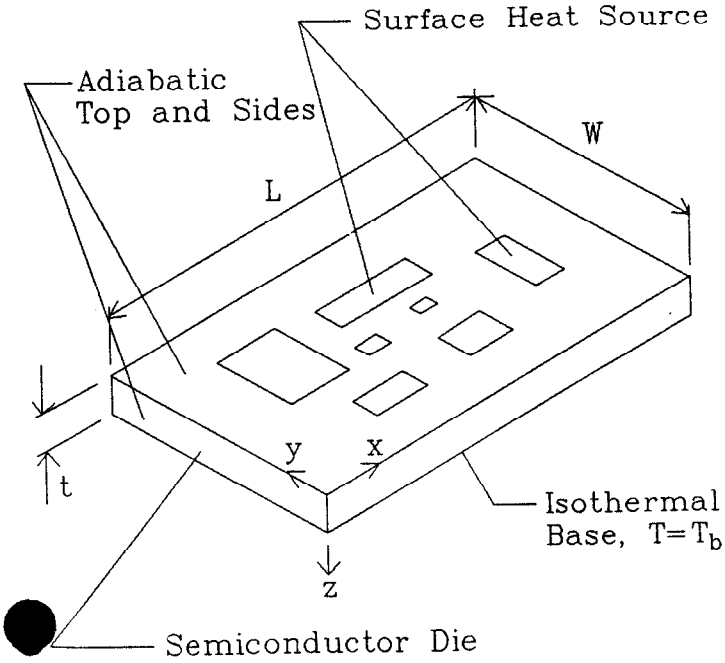

Figure 6: Model for Heat Conduction in Semiconductor Die

$$\nabla \cdot (k(T)\nabla T) = 0 \tag{9}$$

$$-k(T(x,y,0))\frac{\partial T}{\partial z}(x,y,0) = q(x,y) \tag{10}$$

$$\frac{\partial T}{\partial x}(0,y,z,) = \frac{\partial T}{\partial x}(L,y,z) = \frac{\partial T}{\partial y}(x,0,z) = \frac{\partial T}{\partial y}(x,W,z) = 0 \tag{11}$$

$$T(x,y,t) = T_b \tag{12}$$

where $q(x,y)$ is the heat flux distribution applied to the top surface of the die, $k(T)$ is the temperature-dependent thermal conductivity of the die, and T_b is given by

$$T_b = T_\infty + Q\theta_{b-\infty} \tag{13}$$

where T_∞ is some ambient temperature (for convenience T_C can be used), $\theta_{b-\infty}$ is the thermal resistance from the base of the die to T_∞ (package resistance for most microwave devices) and Q is the total heat dissipation

$$Q = \int_{x=0}^{L}\int_{y=0}^{W} q(x,y)dydx \tag{14}$$

The problem described by these equations is one of three-dimensional heat conduction with a non-linearity due to the temperature dependence of the thermal conductivity. It is possible to solve this problem immediately for a given heat flux distribution $q(x,y)$ by using any one of a number of available numerical simulators. This approach has in fact been utilized in previous power transistor studies [8,9]. However, for complex microwave devices and for modern silicon MMIC's, the computational requirements make these fully numerical methods prohibitive for most engineers.

Fortunately, the non-linearity of the homogeneous partial differential equation (eqn. (9)) can always be removed for any $k = k(T)$ by using the Kirchoff transformation [10]. However, non-linear boundary conditions due to $k = k(T)$ are not always linearized by this transformation. The procedure starts by defining a new dependent variable or transformed temperature

$$U = \int_{T_{ref}}^{T} \frac{k(T')}{k(T_{ref})}dT' \tag{15}$$

where $U = U(T)$ only and T_{ref} is some arbitrary reference temperature. For convenience T_{ref} is assumed to be the ambient temperature T_∞ throughout this work.

Application of Leibnitz' Rule for differentiation of an integral gives

$$\nabla U = \frac{k(T)}{k_\infty}\nabla T \tag{16}$$

where $k_\infty = k(T_\infty)$. This can be written as

$$k(T)\nabla T = k_\infty \nabla U \tag{17}$$

which when substituted into eqn. (9) leaves

$$\nabla^2 U = 0 \tag{18}$$

or Laplace's equation.

The non-linear boundary condition of eqn. (10) can be linearized by utilizing eqn. (17) for the transformed temperature to obtain

$$\begin{aligned} k_\infty \frac{\partial U}{\partial z} &= k(T)\frac{\partial T}{\partial z} \\ -k_\infty \frac{\partial U}{\partial z}(x,y,0) &= q(x,y) \end{aligned} \tag{19}$$

For common semiconductors such as silicon and gallium arsenide, excellent correlations of thermal conductivity versus temperature can be made in the form of a simple power law, or

$$k(T) = k_\infty \left(\frac{T}{T_\infty}\right)^p \tag{20}$$

where T is absolute temperature in K. From published data [11] approximate values for silicon and gallium arsenide with $T_\infty = 300\ K$ are

Silicon	—	k_∞	= 1.32	W/cmK
		p	= -1.33	
Gallium Arsenide	—	k_∞	= .40	W/cmK
		p	= -1.06	

With this general power law form for thermal conductivity, U and T are related by

$$U = \frac{T_\infty}{p+1}\left[\left(\frac{T}{T_\infty}\right)^{p+1} - 1\right] \tag{21}$$

$$T = T_\infty \left[1 + (p+1)\frac{U}{T_\infty}\right]^{\frac{1}{p+1}} \tag{22}$$

where $p \neq -1$ has been assumed. The problem can be further simplified for analysis purposes by introducing

$$\phi(x,y,z) = U(x,y,z) - U(x,y,t) \tag{23}$$

or from eqns. (12) and (21)

$$\phi = U - \frac{T_\infty}{p+1}\left[\left(\frac{T_b}{T_\infty}\right)^{p+1} - 1\right] \tag{24}$$

The governing equations now become in terms of the transformed variable ϕ

$$\nabla^2 \phi = 0 \tag{25}$$

$$-k_\infty \frac{\partial \phi}{\partial z}(x,y,0) = q(x,y) \tag{26}$$

$$\frac{\partial \phi}{\partial x}(0,y,z) = \frac{\partial \phi}{\partial x}(L,y,z) = \frac{\partial \phi}{\partial y}(x,0,z) = \frac{\partial \phi}{\partial y}(x,W,z) = 0 \tag{27}$$

$$\phi(x,y,t) = 0 \tag{28}$$

The problem posed by eqns. (25)–(28) requires a linear three-dimensional solution to Laplace's equation in a rectangular prism with one non-homogeneous boundary condition. Many existing numerical techniques and even the classical method of separation of variables can be used to solve this problem. However, all of these methods would suffer computationally due to the complexity of $q(x,y)$ in eqn. (26) for large-scale systems with many active heat sources. In this work an alternative method is proposed based on the Method of Infinite Images [7]. Image techniques have traditionally been used extensively to develop solutions to Laplace's equation in semi-infinite and finite domains and image methods date back over a hundred years to Maxwell. The solution begins by noting that with reference to Figure 7, eqn. (25) is satisfied by the relationship

$$\phi(x,y,z) = \frac{q_n}{2\pi k_\infty}\int_{A_n}\frac{dA}{\rho} \tag{29}$$

where 'n' denotes the n^{th} source of N discrete, rectangular heat sources located on the top surface of the semiconductor die. If N rectangular sources are appropriately chosen in a single plane $z = w = 0$, then the boundary condition of eqn. (26) can also be satisfied exactly. Boundary conditions (27) and (28) for the sides and base of the die are not satisfied, however, and for this purpose images are required.

Consider first the use of image sources as shown in Figure 8 to satisfy eqns. (26) and (28) simultaneously. For a given starting source '0' as shown in Figure 8, the superposition of the image source '1' of negative strength (or a sink) as shown allows the boundary condition on the base of the die (eqn. (28)) to be satisfied exactly. However, the boundary condition of eqn. (26) for the flux-specified plane $z = 0$ is now violated. Thus another image source also of negative strength (image '2') must be superposed as shown in Figure 8 to preserve eqn. (26). Adding image source '2' though once again makes eqn. (28) for the base of the die invalid and thus an image of opposite sign to source '2' must be superposed as shown by image '3' in Figure 8. This pattern of adding an image to satisfy one boundary condition while violating the other continues infinitely in the form of a monotonically convergent series for the potential ϕ within the solution region (the die) shown in Figure 8.

A similar use of images is also utilized to satisfy the requirement of adiabatic sides for the die as expressed by eqn. (27). This goal is accomplished by superposing image sources as shown by the plan view of Figure 9. Note that each image of the starting source has an identical heat flux applied to it and each consists

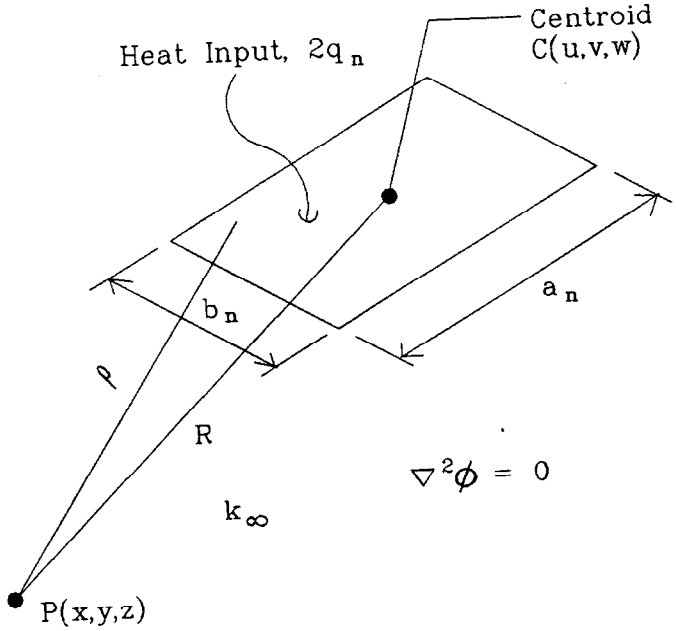

Figure 7: Single Rectangular Heat Source in Infinite Domain

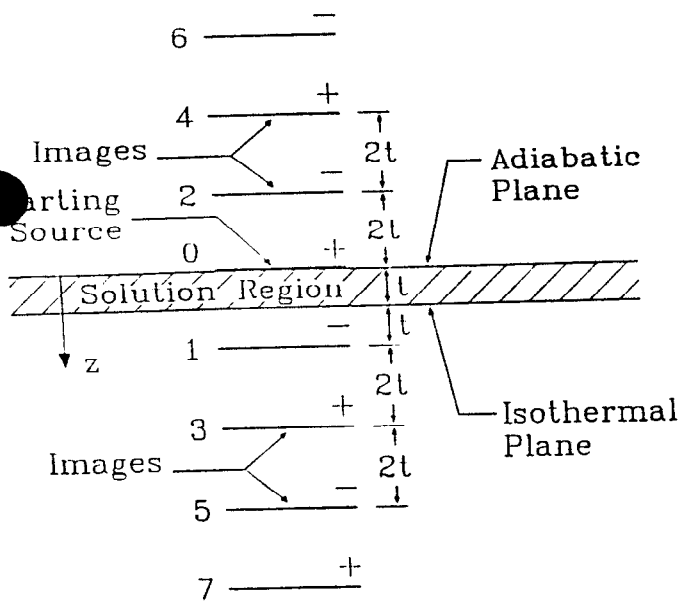

Figure 8: Image Sources Above and Below Die

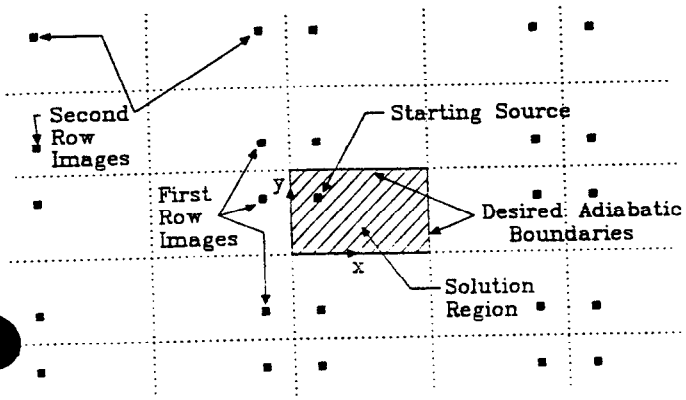

Figure 9: Image Sources in Plane of Die

of a series of infinite images in the z direction as previously described for the starting source. In practice only the first row of images shown in Figure 9 usually makes any significant contribution for the points of maximum temperature rise within the die due to the relative thinness of a typical semiconductor die.

The complete solution can now be written conceptually as

$$\phi = \frac{1}{2\pi k_\infty} \sum_{n=1}^{N} \sum_{i=-\infty}^{\infty} \sum_{j=1}^{\infty} q_n (-1)^i F(x, y, z, u_{nj}, v_{nj}, w_i, a_n, b_n) \quad (30)$$

where $F(\cdot)$ represents a temperature rise influence coefficient due to an individual source. By assuming that rectangular sources are used, F is then a function only of the coordinates of the desired point $P(x, y, z)$, the coordinates of the centroid of the source or image $C(u_{nj}, v_{nj}, w_i)$, the length a_n and width b_n of the n^{th} discrete rectangular surface heat source in the system. N represents the number of active areas on the surface of the semiconductor die and can potentially range from one to several thousand. The first infinite summation ($i = -\infty$ to ∞) represents the images above and below the die and the starting source ($i = 0$). In practise only a few terms in this summation are required for convergence after application of the Euler series transformation [12]. The second infinite summation ($j = 1$ to ∞) refers to the images shown in Figure 9 which usually only contribute significantly from a few in the first row.

Efficient evaluation of the influence coefficient F in equation (30) is extremely important to obtain fast computer execution time for the image methodology. This is accomplished by deriving very simple algebraic expressions for F based on the Surface Element Method [6]. This method has its roots in the classical mathematics of Newtonian potential theory and originally appeared in the early 19$^{\text{th}}$ century work of MacCullagh.

The simple expressions which together comprise an exact analytical solution to the non-linear heat conduction model shown in Figure 6 have been coded in Microsoft BASIC on an IBM-PC along with a graphical, menu-driven user interface. Execution times for most microwave bipolar problems of interest are only minutes or less.

Correlation of Analysis and Experiment

Obviously some experimental validation must be made to have faith that results predicted by THEATRIC will correlate with real thermal behaviour of microwave devices. In addition, the coding of THEATRIC should be verified. In [3] consideration of difficult (for image solutions) limiting cases showed that THEATRIC was coded correctly and does in fact represent an exact solution (to within numerical accuracy) of the thermal model for a semiconductor die as shown in Figure 6. Experimental verification was also given in [3] by comparing THEATRIC predictions to results obtained using LCT on a large bipolar transistor.

Further experimental validation of THEATRIC is presented here for a much smaller geometry microwave device measured by LCT under more controlled conditions and with a larger temperature rise from case to junction. The device measured is the discrete microwave bipolar transistor discussed previously, the Avantek 414 in the 230 mil BeO flange package. The die which measures $305 \times 305 \times 114\ \mu m$ has its entire active heat generation area located centrally in a $60 \times 25\ \mu m$ region. The device was coated with an LCT mixture of NI transition at 100 $°C$ (373 K) and the fixture was adjusted such that T_C remained at 42.7 $°C$ throughout the experiment. With the collector-emitter bias fixed at $V_{CE} = 8\ V$, varying the collector current I_C between 60 and 70 mA (or Q from 480–560 mW) permitted measurements of the 100 $°C$ contour on the active device region as a function of power dissipation.

Although the thermal resistance from the base of the 414 die to the case temperature T_C is small relative to the resistance within the die, its value is still required for input as $\theta_{b-\infty}$ (eqn. (13)) to THEATRIC. Since the die dimensions are small relative to the beryllia base in the package, a good estimate of $\theta_{b-\infty}$ is then [6]

$$\theta_{b-\infty} \approx \frac{.44}{k\sqrt{A_b}} \quad (31)$$

where k is the thermal conductivity of the package base (for beryllia $k \approx 2.5\ W/cm°C$) and A_b is the area of the base of the die. For the 414 die in the 230 mil BeO flange package, eqn. (31) predicts

$$\theta_{b-\infty} \approx 6 \qquad °C/W \quad (32)$$

With this value of $\theta_{b-\infty}$ given as input to THEATRIC along with $T_\infty = T_C = 42.7\ °C$, the program was run with three different values of total power dissipation corresponding to the experimental measurements shown in Figures 10–12. THEATRIC generated isothermal contours for the active region of the die as shown in Figures 10–12. The agreement between THEATRIC and the LCT measurements is excellent. For the first case of $Q = 489\ mW$, THEATRIC predicts the center of the active region at 100 $°C$ and the 99 $°C$ (372 K) contour in Figure 10 is seen to be nearly identical to 100 $°C$ (373 K) contour in the LCT measurement – an insignificant error of less than 2%. In

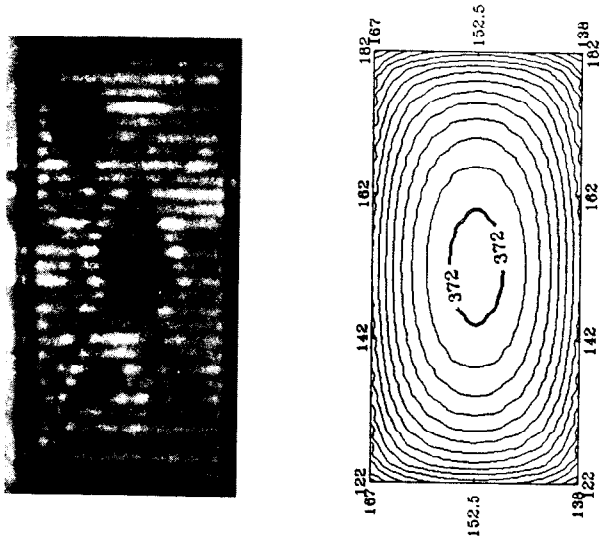

(i) (ii)

Figure 10: Comparison of 100 °C (373 K) Contour on Avantek 414 Die as measured by LCT (i) and as predicted by THEATRIC (ii) for $Q = 489\ mW$

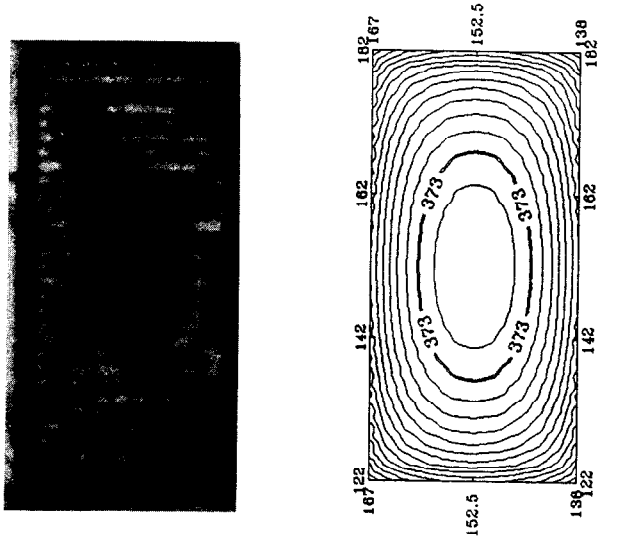

(i) (ii)

Figure 11: Comparison of 100 °C (373 K) Contour on Avantek 414 Die as measured by LCT (i) and as predicted by THEATRIC (ii) for $Q = 521\ mW$

Figure 11 the results at $Q = 521\ mW$ show excellent agreement again with only minor differences between the 100 °C contour of the LCT measurement and the THEATRIC prediction. Note that the unlabeled contours on the THEATRIC results in Figures 10–12 are on 2 °C intervals. Note also that the rectangular border of the THEATRIC results corresponds approximately to the dark rectangular outline of the active device area in the LCT photographs. At the highest power dissipation of $Q = 545\ mW$, Figure 12 again shows good agreement between THEATRIC and LCT measurement. In general Figures 11 and 12 show that the real device has its isotherms closer to the center than predicted by THEATRIC. The reason stems essentially from the first-order

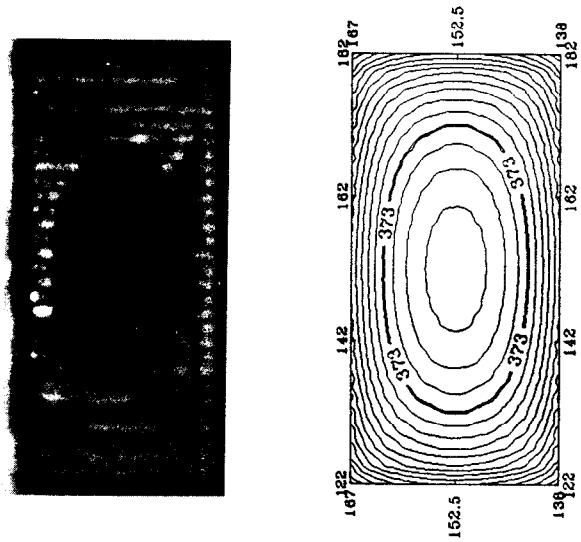

(i) (ii)

Figure 12: Comparison of 100 °C (373 K) Contour on Avantek 414 Die as measured by LCT (i) and as predicted by THEATRIC (ii) for $Q = 545\ mW$

relationship between current density (and hence power dissipation density) and local junction temperature as evident from eqn. (1). Since V_G in eqn. (1) is greater than V_{BE} for silicon devices, the current density increases near the center of the active emitter area (where local T_j is hotter) for fixed V_{BE} and thus does not produce the isotherm growth toward the edges as predicted by THEATRIC which assumed uniform power density.

In addition to these results, THEATRIC has also been shown to compare favourably with other LCT results taken on other microwave bipolar transistors and MMIC's at different NI transition temperatures from 87 °C to 150 °C.

Application to Device Optimization

With silicon MMIC's there are many different layout or circuit design options which can impact on the thermal characteristics of a new product. THEATRIC can be used to study the trade-offs between obtaining uniform junction temperatures versus circuit performance when selecting optimum device biases (or power dissipation) and layout positions with minimal parasitic capacitance. Highly non-uniform junction temperatures imply high "apparent" θ_{jc} for reliability purposes and can lead to problems of device V_{be} matching for given collector currents I_C (recall relationship of V_{be} and T_j as given by eqn.(1)).

A simple practical example of a manufacturing trade-off versus thermal resistance is currently of interest at Avantek due to the productivity enhancement of using 3" wafers instead of 2". The problem which has arisen from this switch is that backlapping of the wafers to the previous specification of 114 μm or 4.5 mil leads to excessive wafer breakage during saw and assembly. Since wafer stiffness is approximately proportional to the cube of the thickness, backlapping the wafers down less, for example to 152 μm or 6 mil, can greatly reduce this problem. However the thicker final dice produced will have a higher thermal resistance due to heat conduction within the die. This in turn could lead to reduced long term reliability and/or a restriction on acceptable case temperatures especially for plastic packages.

With THEATRIC it is relatively simple to study the impact of die thickness on junction temperature for any discrete device

or MMIC for a given package type, case temperature and power dissipation. For example, results are given in Figure 13 for the maximum junction temperature versus die thickness on the 414 discrete device and the INA-01 silicon MMIC both in 230 mil BeO flange packages. The conditions are $T_C = 125\ ^\circ C$ and power dissipation corresponding to normal recommended bias conditions (200 mW for the 414 and 230 mW for the INA-01). Figure 13 shows that increasing die thickness has only a minor effect on peak T_j especially for a small increase of 152 μm from 114 μm. For this proposed increase in die thickness the peak junction temperature increases only about 1 $^\circ C$ and θ_{jc} about 5 % for the 230 mil BeO flange package. For other packages the relative increase in θ_{jc} will be even less although the temperature increase remains about the same.

Application to Reliability Studies

For most microwave bipolar transistors and MMIC's in hermetic ceramic packages, the major reliability issue is electromigration in the metallization on chip. At normal operating temperatures and currents failures occur only over long periods of time. However, since electromigration has been shown to be exponentially related to temperature, the reliability of microwave products can be studied in shorter periods of time by "stressing" the devices at normal bias conditions (and hence current densities in the metallization) but with elevated temperatures. Typically a finite lot of 30–100 components are stressed at T_j of 225–290 $^\circ C$ for 1000–4000 hours (about 6–24 weeks). Failures within the first 24 hours are usually discounted as "infant mortalities". The median time to failure (MTF) at some junction temperature T_{j0} is then related to the junction temperature of the stressed components, T_{j_s}, according to

$$\mathrm{MTF}(T_{j0}) = \frac{t_s}{2f} \exp\left[-\frac{E_a}{k}\left(\frac{1}{T_{j_s}} - \frac{1}{T_{j0}}\right)\right] \qquad (33)$$

where t_s is the length of time the components are stressed at junction temperature T_{j_s}, f is the fraction that fail in time t_s, E_a is the electromigration activation energy for the metal, and k is Boltzmann's constant. The junction temperature T_{j_s} for the reliability study is calculated from

$$T_{j_s} = T_C + \theta_{jc} Q \qquad (34)$$

where Q is the total power dissipation on the die.

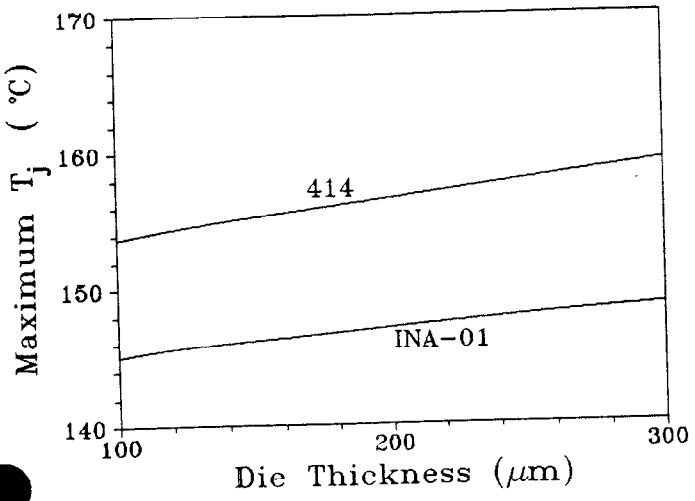

Figure 13: Maximum Junction Temperature on Avantek 414 and INA-01 versus Die Thickness

Because of the exponential relationship in eqn. (33), predictions of MTF at a given T_{j0} are obviously very sensitive to E_a and T_{j_s}. The activation energy E_a can be calculated empirically by stressing different lots of identical components at different T_{j_s} and then using regression to obtain a best fit for E_a in eqn. (33) under the assumption that the same MTF should be predicted regardless of the T_{j_s} of the study. However, for both calculating E_a and subsequently MTF with eqn. (33), substantial errors can arise if the value of θ_{jc} in eqn. (34) was measured at substantially lower temperatures but not corrected for the effect of decreased silicon thermal conductivity at high temperatures.

For example, consider some reliability data gathered recently for the Avantek INA-01 silicon MMIC which has been described previously in this work. LCT measurements of this product in the 230 mil flange package used in the reliability study predict $\theta_{jc} = 80\ ^\circ C/W$ based on the temperature near the ends of the emitter fingers (a point of maximum current density and many electromigration failures). With this value of θ_{jc} the MTF for a junction temperature of 150 $^\circ C$ is predicted from measurements at $T_C = 260\ ^\circ C$ to be 1.0×10^6 hours for devices which due to a mask problem (now corrected) had metallization only 70 % as thick as that normally used. This MTF value would be considered marginal by industry standards but in fact is misleading because θ_{jc} at $T_C = 260\ ^\circ C$ is really substantially higher. At a junction temperature of about 100 $^\circ C$, THEATRIC predicts $\theta_{jc} = 80\ ^\circ C/W$ for the INA-01 based on the contour size of the LCT measurement which agrees perfectly. At $T_C = 260\ ^\circ C$ THEATRIC shows $\theta_{jc} \approx 125\ ^\circ C/W$. With this value of thermal resistance for the reliability study conditions, the same data now extrapolates to an MTF of 1.6×10^6 hours at 150 $^\circ C$ junction temperature.

Conclusions

The major goals of this paper have been to discuss the thermal issues which face the silicon bipolar microwave industry, to describe some of the experimental and modeling techniques used to characterize thermal resistance, and to illustrate how these techniques are applied to actual devices.

In summary, the liquid crystal transition (LCT) technique has been generally found to be much more accurate than infrared (IR) microscopy for microwave applications because of its increased resolution. Modern bipolar devices that operate at microwave frequencies have very narrow emitters located closely together with high local power dissipation densities. As a result the ability of the LCT method to resolve thermal gradients across distances of 2–4 μm makes it a valuable tool for thermal characterization. Considerable attention has also been directed in this paper towards the ideal junction law method of determining θ_{jc} as an alternative approach for plastic packages. Although it is recognized that this method is not applicable for many power bipolar applications where θ_{jc} has limited meaning anyways, the addition of Early effect to the experimental procedure gave excellent agreement with LCT results for a real microwave bipolar device in two different ceramic packages.

In addition to experiments, the basic theory behind a novel analytical modeling tool, THEATRIC, for thermal characterization of microwave bipolar transistors and MMIC's was also presented. This engineering software package addresses the problem of non-linear, three-dimensional heat conduction within a semiconductor die. THEATRIC predictions based on published values of silicon thermal conductivity versus temperature were in good agreement with experimental results obtained for microwave transistors and MMIC's using LCT.

The combination of analysis and modeling can help solve a

variety of thermal issues for the microwave industry. Examples of product optimization trade-offs were discussed and illustrated using THEATRIC. In addition the importance of correctly extrapolating θ_{jc} measurements to higher temperatures was demonstrated for a reliability study on a silicon MMIC.

References

[1] Negus, K.J., Yovanovich, M.M. and Roulston, D.J., 1987, "An Introduction to Thermal-Electrical Coupling in Bipolar Transistors," presented at the Second ASME-JSME Thermal Engineering Joint Conference, Honolulu, HA.

[2] Negus, K.J. and Yovanovich, M.M., 1987, "Thermal Computations in a Semiconductor Die Using Surface Elements and Infinite Images," *Proceedings of the International Symposium on Cooling Technology for Electronic Equipment*, Pacific Institute for Thermal Engineering, Honolulu, HA, pp. 474–485.

[3] Negus, K.J., 1988, "Thermal and Electrical Modeling of Bipolar Devices," Ph.D. Thesis, Dept. of Mechanical Engineering, University of Waterloo, Waterloo, CANADA.

[4] Sze, S.M., 1981, *Physics of Semiconductor Devices*, Wiley-Interscience, New York.

[5] Getreu, I., 1976, *Modeling the Bipolar Transistor*, Tektronix Part No. 062-2841, Tektronix, Inc., Beaverton, OR.

[6] Yovanovich, M.M., Thompson, J.C. and Negus, K.J., 1983, "Thermal Resistance of Arbitrarily Shaped Contacts," Third International Conference on Numerical Methods in Thermal Problems, Seattle, WA.

[7] Negus, K.J., Yovanovich, M.M. and DeVaal, J.W., 1985, "Development of Thermal Constriction Resistance for Anisotropic Rough Surfaces by the Method of Infinite Images," ASME Paper No. 85-HT-17, 23rd ASME-AIChE National Heat Transfer Conference,Denver, CO.

[8] Latif, M., 1979, "A Numerical Study of Transistor Behaviour Including Thermal Effects," Ph.D. Thesis, Dept. of Electrical Engineering, University of Waterloo, Waterloo, CANADA.

[9] Opal, A., 1984, "Thermal Modelling of Bipolar and MOSFET Devices," M.A.Sc. Thesis, Dept. of Electrical Engineering, University of Waterloo, Waterloo, CANADA.

[10] Osizik, M.N., 1980, *Heat Conduction*, Wiley-Interscience, New York.

[11] Maycock, P.D., 1967, "Thermal Conductivity of Silicon, Germanium, III-V Compounds and III-V Alloys," *Solid-State Electronics*, Vol. 10, pp. 161–168.

[12] Olver, F.W.J., 1974, *Asymptotics and Special Functions*, Academic Press, New York.

[13] Cohen, B.G., 1977, "Infra-Red Microscopy for Evaluation of Silicon Devices and Die-Attach Bonds," *Multidisciplinary Microscopy*, SPIE Vol. 104, pp. 125–131.

[14] Channin, D.J., 1974, "Liquid-Crystal Technique for Observing Integrated Circuit Operation," *IEEE Transactions on Electron Devices*, Vol. ED-21, No. 10, pp. 650–652.

[15] Oettinger, F.F., Blackburn, D.L. and Rubin, S., 1976, "Thermal Characterization of Power Transistors," *IEEE Transactions on Electron Devices*, Vol. ED-23, No. 8, pp. 831–838.

[16] Van Meter, J.P., 1973, "Chemistry of Liquid Crystals," *Eastman Organic Chemical Bulletin*, Vol. 45, No. 1.